Applications in Engineering Science 9 (2022) 100077

Contents lists available at ScienceDirect

Applications in Engineering Science

journal homepage: www.elsevier.com/locate/apples

Durability of fibre-reinforced cementitious composites (FRCC) including recycled synthetic fibres and rubber aggregates

Cesare Signorini [a,b], Andrea Nobili [c,d,*]

[a] Interdepartmental Research Centre CRICT, University of Modena and Reggio Emilia, via Vivarelli 10, 41125 Modena, Italy
[b] Institute of Construction Materials, Technical University Dresden, Georg-Schumann-Str. 7, 01187 Dresden, Germany
[c] Department of Engineering "Enzo Ferrari", University of Modena and Reggio Emilia, via Vivarelli 10, 41125 Modena, Italy
[d] Interdepartmental Research Centre "En&Tech", University of Modena and Reggio Emilia, P.le Europa 1, 42124 Reggio Emilia, Italy

ARTICLE INFO

Keywords:
Ageing
Fibre-reinforced cementitious composites
Recycled synthetic fibres
Recycled aggregates

ABSTRACT

We discuss mechanical performance of fibre-reinforced cementitious composites under exposure to four aggressive environments, namely alkaline, saline, sulphuric acid and distilled water immersion. A standard commercial Portland cement based matrix is considered alongside its lightweight modification wherein quarzitic sand is partially replaced by recycled rubber crumbs. Also, virgin polypropylene fibres are contrasted to PP+PET blended fibres where the PET fraction is obtained from recycling food packaging waste. Performance is assessed in bending as well as in compression. We find that recycled based specimens perform surprisingly well and that exposure to the aggressive environments mainly affects the matrix and it is not necessarily more detrimental to the lightweight partially recycled phase. A one-way analysis of variance (ANOVA) confirms the statistical significance of the results, which fully support the idea that the adoption of a substantial recycled fraction in construction materials still allows for high performance and durability standards.

1. Introduction

Fibre-reinforced cementitious composites (FRCCs) encompass a large class of materials whose properties are strongly dependent on the successful matching between the matrix and the reinforcing phase (Bentur and Mindess, 2006). In particular, adopting short randomly dispersed fibres (such as glass, steel, polypropylene etc.) in a cementitious matrix is a well established technique, that is currently widespread in the construction sector. Indeed, a vast body of experimental knowledge concerning the mechanical behaviour of FRCC has been developed over the decades alongside models thereof (Whitney et al., 1982; Yang and Li, 2010; Sorzia et al., 2019). Essentially, FRCC's value lies in its greatly enhanced toughness, owing to friction sliding of the fibres at the post-cracking stage of the brittle matrix. A sizeable body of literature is devoted to FRCC materials, especially adopting short randomly dispersed steel fibres, whose study dates back to the early 1970s and stands in ideal continuity with the development of traditional reinforced concrete (RC) (Almansa and Canovas, 1970; Tardiff Jr., 1973; Naaman and Shah, 1976). In fact, much of these pioneering investigations heavily draw over the established knowledge of rebar interaction with concrete. In more recent times, the use of synthetic fibres in the place of steel has gained momentum, in an attempt to circumvent the much undesired effects of steel oxidation (Rider and Heidersbach, 1980), for an account of which, the interested reader is referred to the recent review by Marcos-Meson et al. (2018). Besides, FRCC vulnerability to high temperature and fire exposure is still being investigated, especially in the form of concrete *spalling*, to which high-strength conglomerates are particularly susceptible (Peng et al., 2006; Zhang et al., 2020). Clearly, when compared with steel, plastic fibres are more durable and impart remarkable anti-spalling properties to the composite (Dong et al., 2008). A recent review of the use of macro plastic fibres in concrete is given by Yin et al. (2015).

The use of polymeric materials for manufacturing reinforcing fibres aimed at FRCC paves the way for a sustainable material selection process, that allows for recycled products. Many recent studies investigate the possibility of including end-of-life fibres from different sources, such as carpets (Wang, 1995), industrial waste (Meddah and Bencheikh, 2009) and plastics (Gu and Ozbakkaloglu, 2016). This approach brings important advantages in terms of environmental sustainability and resource preservation, as demonstrated by Marinelli et al. (2021) through life-cycle assessment (LCA) of FRCC obtained from recycling sport facilities. Signorini and Volpini (2021) tested various FRCC systems with recycled plastic fibres and filaments obtained with limited industrial re-processing of the raw materials, showing that mechanical performance can be comparable with that of virgin fibres. Fraternali et al.

---

* Corresponding author at: Department of Engineering "Enzo Ferrari", University of Modena and Reggio Emilia, via Vivarelli 10, 41125 Modena, Italy.
E-mail address: andrea.nobili@unimore.it (A. Nobili).

https://doi.org/10.1016/j.apples.2021.100077
Received 4 November 2021; Accepted 8 November 2021

(2011) show that recycled PET fibres in concrete foster a significant improvement in the thermo-mechanical response, compared to plain concrete. Indeed, strain-hardening is observed in the case of PP fibres. Results follows on the wake of the experiments previously conducted by Ochi et al. (2007) adding draw-wire fibres obtained from recycling PET bottles to concrete at 3% dosage. Similarly, Foti (2013) consider reinforcing concrete with platelets obtained simply cutting PET bottles and find good adherence with the matrix. Precisely this issue is elaborated upon by Marthong and Sarma (2016) with mixed results. Adoption of recycled lightweight inert materials, such as plastics, is proven to impart to the composite low specific weight and additional beneficial properties, such as thermal (Medina et al., 2017; Wang and Du, 2020) and acoustic (Holmes et al., 2014; Medina et al., 2016; Zhang and Poon, 2018) insulation capabilities. In the recent literature review by Li et al. (2020), the use of rubber aggregates in concrete is addressed and the environmental implications thereof evaluated.

The issue of fibre durability is of critical importance, especially when recycled materials are concerned (Larsen and Krenchel, 1990). In fact, this concern is especially relevant when considering PET reinforcement, which is largely susceptible to the alkaline environment of concrete (Silva et al., 2005). Although some specific studies are available, to the best of the authors' knowledge, a comprehensive investigation of ageing in different aggressive environments for FRCC including both recycled fibres and recycled aggregates is missing. This topic is investigated by Won et al. (2010) where concrete reinforced with PET fibres is subjected to accelerated ageing with different immersion times in various aggressive solutions. The effect of salt water, alkaline, and acid exposure are evaluated. Acid and strongly alkaline solutions deteriorate the surface of the fibres and, as it may be expected, the damage, which appears already after 30 day immersion, increases with the soaking time. Conversely, the saline environment does not seem to negatively affect the recycled PET fibres. However, only compressive performance indices are investigated (i.e. elastic modulus and compressive strength), and no consideration is given to bending. Silva et al. (2005) investigate the degradation of recycled PET fibres in an ordinary Portland cement (OPC) mortar after 164 days and in several alkaline solutions for 150 days at 3 different temperatures. Diffuse degradation due to the interaction with the alkaline medium emerges from this study. Several other contributions support the idea that long-term performance of PET fibres in the alkaline environment is questionable (Benosman et al., 2011, 2013).

In this study, we investigate mechanical performance of FRCC prisms in which partially recycled draw-wired cylindrical synthetic fibres act as the dispersed reinforcement phase. Fibres are obtained from a blend of polyethylene and polyethylene terephthalate, PE-PET, derived from processing low-grade food packaging, that is mixed with virgin polypropylene, PP. Fibres are dispersed in either a mineral aggregate standard matrix, which acts as reference, or a lightweight matrix obtained by partially replacing quartz sand with recycled styrene-butadiene crumb rubber. 60 day exposure in four different aggressive environments, namely saturated humidity conditions, sulphuric acid, saline and alkaline, is considered. Performance is assessed in terms of surface modification as well as flexural and compressive strength decay. An analysis of variance (ANOVA) of the results is conducted to assess the statistical significance of the decay profiles.

2. Materials and methods

2.1. Materials

Draw-wire partially recycled fibres with cylindrical shape are made from mixing virgin polypropylene (PP) with a blend of polyethylene (PE) and polyethylene terephthalate (PET) in the form of low-grade flakes obtained from industrial processing of food packaging (Signorini and Volpini, 2021). The nozzle diameter is 750 μm. For the purpose of comparison, plain vanilla PP fibres are also manufactured with the same geometrical characteristics. Fibres are shown in Figs. 1(a–b). Optical inspection reveals that fibres present a smooth surface, without any significant damage due to manufacturing.

Table 1
Formulation of the embedding media.

Matrix	OPC [%]	MA [%]	RRA [%]	w/c ratio
PC	23	77	0	0.43
LWC	23	58	19	0.43

OPC = Ordinary Portland Cement 42.5R
PC = plain conglomerate, LWC = lightweight conglomerate, MA = Mineral Aggregates, RRA = Recycled Rubber Aggregates.

For the matrix, we consider a customised screed fine-grained concrete. Alongside the standard formulation, named PC, a modified matrix is considered wherein a portion of virgin mineral aggregates (namely quartzitic river sand) is replaced by recycled styrene-butadiene rubber aggregates, SBR, as in Fig. 1(c). Conversely, the binder content and the w/c ratio are the same for both matrices. The modified matrix possesses features resembling lightweight concrete, whence the label LWC. Main composition details are reported in the details in Table 1.

2.2. Specimen manufacturing

First, ordinary Portland concrete (OPC) is mixed with aggregates and fibres. Solid phases are gently stirred to promote uniform fibre distribution. Then, water is added progressively and the paste is left to homogenise for 3 min. To perform three-point bending (3PB) tests, prismatic beams are cast out of lubricated plastic moulds, compliant with the guidelines (UNI EN 1015-11, 2007) concerning the assessment of flexural properties of hardened cement-based conglomerates. Specimen dimensions are 4 × 4 × 16 cm. After being stripped (2 days later), specimens are left to cure for further 26 days tightly wrapped in a polypropylene bag in saturated humidity conditions. After curing, specimens are either exposed to the aggressive environments, as hereinafter detailed, or left to harden at laboratory conditions for 60 days.

2.3. Experimental programme and ageing protocols

The experimental programme is summarised in Table 2. For the sake of comparison, 5 accelerate ageing protocols are considered which follow the prescriptions given by Won et al. (2010). Specifically, the following solutions are prepared:

- *Saline (SL)*: an aqueous solution of sodium chloride (NaCl, 3.5%w.) that simulates the average salt content of seawater, according to ASTM D 1141 (2013) and also adopted in a recent paper by Signorini and Nobili (2021) investigating textile-reinforced mortar composites;
- *Alkaline (AL)*: an aqueous solution of calcium hydroxide ($Ca(OH)_2$, 0.16%), sodium hydroxide (NaOH, 1%), and potassium hydroxide (KOH, 1.4%). The pH of the solution is 12.6 (Won et al., 2010);
- *Sulphuric acid (SA)*: a 3% aqueous solution of sulphuric acid (H_2SO_4) (Won et al., 2010);
- *distilled water immersion (HU)*: used as comparison to distinguish between the effects of water and of the reactants in the other solutions;

It is emphasised that, to better focus on the damaging mechanism, both bare fibres and FRCC specimens are immersed in the aggressive solutions. FRCC specimens are exposed for 60 days at 23 °C in a Peltier driven climatic chamber (Memmert). In contrast, fibres are exposed for 30 days and then their surface is optically investigated, in order to detect early superficial damage. This intermediate investigation is intended to be compared with the damage scenario described in Won

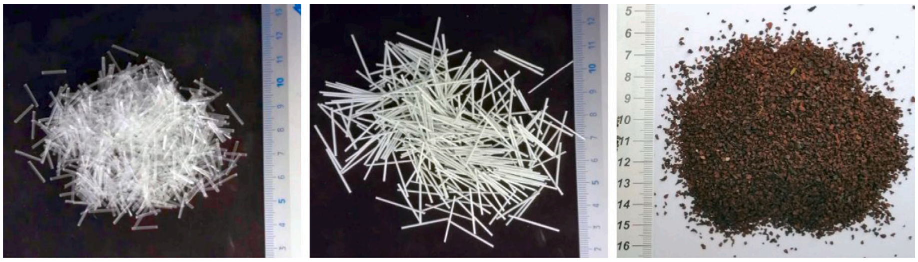

(a) PP fibres (b) RPPP fibres (c) RRA

Fig. 1. Fibres (a,b) and recycled rubber aggregates (c).

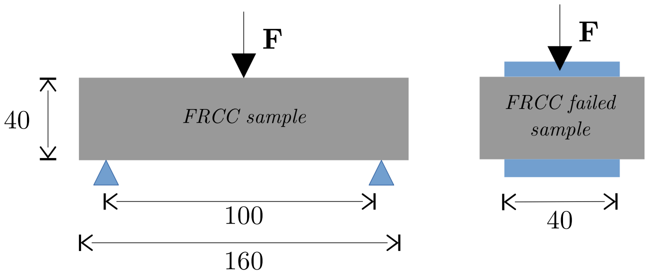

Fig. 2. Schematic front-view of 3PB and compression test configurations.

Table 2
Experimental programme *(3PBT = 3-point bending test; MCT = monotonic compression tests)*.

Test	Matrix	Fibres	Envs.	Specs.
3PBT	plain (PC)	PP	C/HU/SA/AL/SL	4 for each env.
		RPPP	C/HU/SA/AL/SL	4 for each env.
	lightweight (LWC)	PP	C/HU/SA/AL/SL	4 for each env.
		RP-PP	C/HU/SA/AL/SL	4 for each env.
MCT	lightweight (LWC)	PP	C/HU/SA/AL/SL	4 for each env.
		RP-PP	C/HU/SA/AL/SL	4 for each env.

et al. (2010). Control specimens, labelled C, are equally cured for 60 days, although in air at laboratory conditions. Air curing was preferred to water curing since it reproduces the curing procedure generally adopted in standard practice.

2.4. Characterisation methods

To characterise the aggregates, the particle size distribution curve is obtained following the standard guidelines and referring fractions passing through sieves. Besides, compositional investigation is carried out through Fourier-Transform Infrared Spectroscopy in attenuated total reflection mode (FTIR-ATR), by means of a Vertex70 Bruker spectrometer. Fibres are characterised by scanning electron microscopy (SEM) to detect possible morphological variations and superficial damaging due to immersion in the aggressive solutions. FRCC mechanical performance is assessed through three-point bending (3PB) tests on unnotched prismatic specimens at prescribed displacement. Tests are carried out in an Instron 5567 universal testing machine (UTM) equipped with a 30 kN load cell. Two lower anvils are attached to the fixed cross-bar and act as supports, whereas the moving knife loads the specimen at the mid-span with fixed speed at 1 $\mathrm{mm\,min^{-1}}$.

Compression tests are performed on the two halves of the failed specimens. In this case, the same UTM is equipped with two stainless steel plates and specimens are tested on a 40-mm-sided square load imprint by using two steel adaptors. Again, the prescribed displacement in the compression tests is set to 1 $\mathrm{mm\,min^{-1}}$. For comparison purposes, only LWC specimens are characterised in compression test as their strength is compatible with the adopted load cell. The schematic of the test configurations are reported in Fig. 2.

3. Results

3.1. Characterisation of aggregates and fibres

Fig. 3 compares particle size distribution of mineral aggregates (as provided by the manufacturer) with that of recycled rubber aggregates. By partially replacing the former with the latter, the resulting mixture becomes coarser, in the sense that porosity is increased. Indeed, at 0.5 mm of particle equivalent diameter, only around 20% of recycled SBR aggregates (RRA) passes through the corresponding sieve, whereas for quartzitic sand (MA), the passing fraction is slightly below 80%. This, in turn, explains the lightweight character of the modified mixture.

A similar comparison, although this time in terms of FT-IR spectra, is presented in Fig. 4. As expected, quartz sand presents a wide absorbance peak at 3368 $\mathrm{cm^{-1}}$, due to O-H interactions ascribed to moisture. Besides, the typical peaks associated to silica are observed. Briefly, asymmetric and symmetric stretching vibrations of Si-O bonds are obvious around 1000 $\mathrm{cm^{-1}}$ and 775 $\mathrm{cm^{-1}}$, respectively, whereas Si-O symmetric bending vibrations can be detected at 693 $\mathrm{cm^{-1}}$. On the other hand, SBR recycled aggregates present a more complicated absorbance pattern, similar to the findings reported by Luna et al. (2020). Indeed, typical peaks associated to rubber appear at around 752 $\mathrm{cm^{-1}}$, and in the range between 900 $\mathrm{cm^{-1}}$ and 1000 $\mathrm{cm^{-1}}$, which indicate the presence of various groups, like 1,4 cis-butadiene, 1,4 trans-butadiene, and 1,2-butadiene. Also, the peak at 1636 $\mathrm{cm^{-1}}$ corresponds to stretching vibrations of CH_2 and CH_3 units. Finally, evidence for the presence of styrene is given by two clear peaks at 2848 $\mathrm{cm^{-1}}$ and 2916 $\mathrm{cm^{-1}}$, which emerge from elongation of CH units in the styrene aromatic ring (Luna et al., 2020). The presence of various fillers is supported by the observation of several peaks. For example, the presence of talc is attached to the major peak at around 3693 $\mathrm{cm^{-1}}$, that is related to Mg_3OH, while the presence of calcium carbonate is strongly indicated by detection of the typical vibrations of ${CO_3}^{-2}$ at 1419 $\mathrm{cm^{-1}}$ and 874 $\mathrm{cm^{-1}}$), see also Luna et al. (2020).

3.2. SEM investigation of fibres

The effect of accelerated ageing on bare fibres is assessed by Scanning Electron Microscopy (SEM) after 30-day immersion, and it is shown in Figs. 5. PP fibres present a very smooth surface, with characteristic longitudinal grooves formed during the extrusion and drawwiring processes. Remarkably, the surface of partially recycled fibres is rough and uneven, as a consequence of the immiscibility of the polymeric phases in the molten mix, namely PP, PE and PET, which tend to mutually slide during the extrusion process. With regard to aged fibres, no significant variation occurs on their surface, regardless of the exposure and of the fibre composition. As expected, salt water

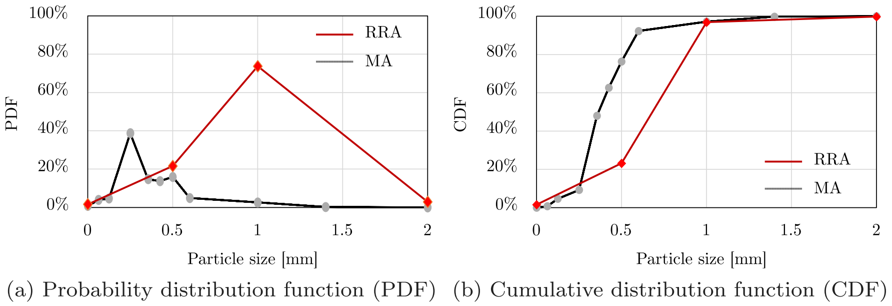

(a) Probability distribution function (PDF) (b) Cumulative distribution function (CDF)

Fig. 3. Particle size distribution of mineral aggregates (MA) and recycled rubber aggregates (RRA).

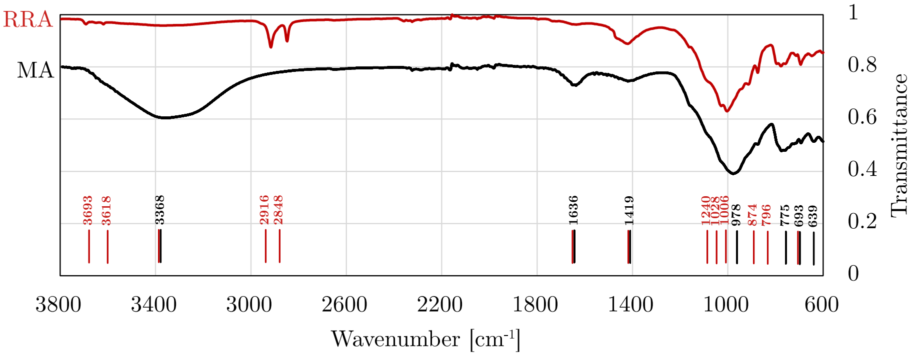

Fig. 4. FTIR-ATR spectrum of quartzitic sand (MA) and recycled SBR aggregates (RRA).

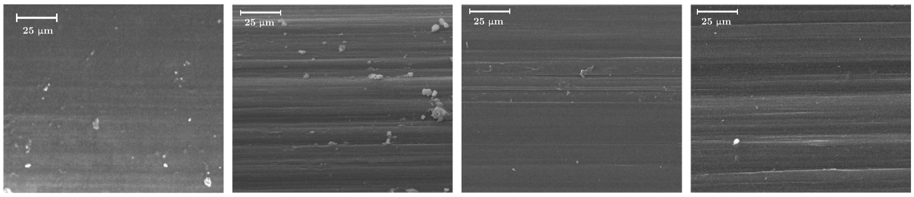

(a) PP-C (b) PP-SL (c) PP-SA (d) PP-AL

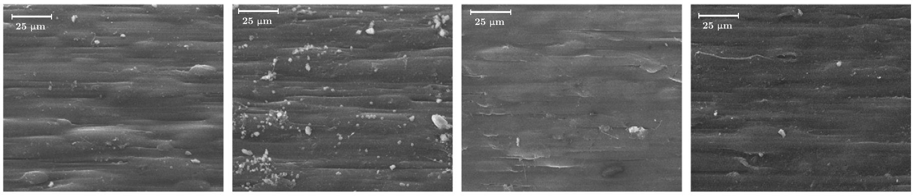

(e) RPPP-C (f) RPPP-SL (h) RPPP-SA (k) RPPP-AL

Fig. 5. Fibre surface after 30-day exposure to saline (SL), sulphuric acid (SA) and alkaline (AL) environment, as it compares to the control group (C).

exposure induces the formation of NaCl crystals on the surface, and this is especially the case for mixed virgin/recycled fibres owing to their rough surface. However, no significant corrosion, pitting or other form of surface damage can be observed, thus fibres appear remarkably stable against direct exposure to the aggressive environments. This outcome is in contrast with the results obtained by Won et al. (2010, Figs. 4–8), who, upon SEM investigation, report diffuse deterioration of pure recycled PET fibres after 30-day exposure to the alkaline as well as to the acid environment. Yet, our results appear in line with the findings given by Ochi et al. (2007), who report no significant detrimental effect on PET fibres by the alkaline environment of concrete. These clashing outcomes may be partly motivated by the importance of the ageing protocol details in connection to the fibre composition and manufacturing process. In any case, they support the need for further investigation in this area.

3.3. *Mechanical performance assessment*

3.3.1. *Strength curves in bending*

Fig. 6 reports the mean stress–strain curves obtained in bending tests, averaging out 4 specimens within each group. Stress is conventionally deduced by Navier's formula. Both standard (PC) and lightweight conglomerates (LWC) are considered. We observe that data scattering is reasonably narrow, especially considering an ageing

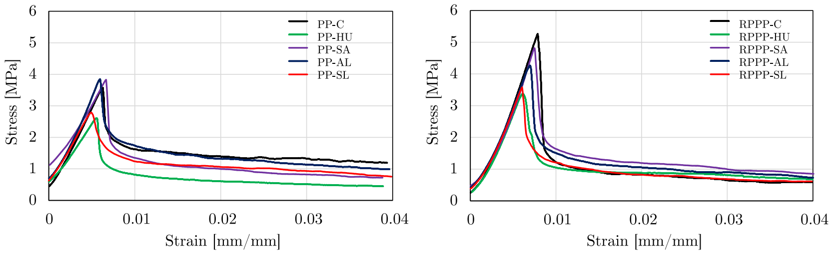

(a) PC + PP fibres (b) PC + RPPP fibres

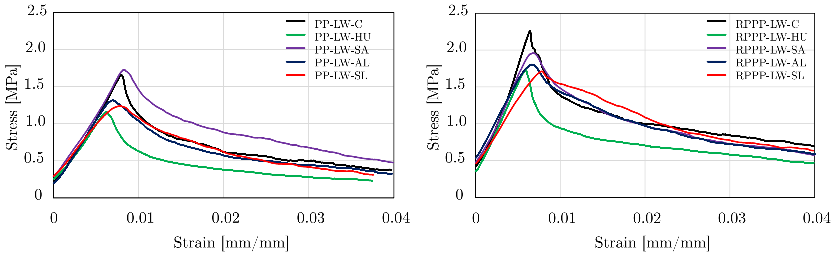

(c) LWC + PP fibres (d) LWC + RPPP fibres

Fig. 6. Strength curve of plain (PC) and lightweight (LW) conglomerates subjected to the aggressive environments (SA — saline, AL — alkaline, SL — sulphuric acid, HU — water immersion) or in the control group (C).

process, and at least comparable with that of similar testing campaigns available in the literature. As expected, all specimens display strain-softening behaviour, with an initial perfectly elastic response up to the first-cracking stress. The sudden stress drop at the end of the elastic stage pin-points the first cracking strength (FCS) of the matrix and it is followed by the crack opening stage. For the standard matrix, the latter occurs at almost constant stress, namely 1 MPa. Remarkably, the presence of recycled aggregates improves strength and decreases scattering, as it may be seen comparing 6(b) with (a) for PC and (d) with (c) for LWC. In contrast, lightweight concrete exhibits lower first cracking stress, due to the weaker matrix, and a mild softening post-peak branch, with no dramatic strength loss at cracking, which is quite beneficial in terms of toughness.

For the purpose of better illustration, the mean first cracking strength (σ_{CR}) and dissipated energy (W_f) at failure, together with ±1 standard deviation intervals, are displayed in the bar-charts of Figs. 7 and 8, respectively. Very remarkably, greater strength is consistently attached to the adoption of partially recycled fibres and recycled rubber aggregates, as opposed to virgin PP fibres. From a general perspective, this outcome appears to contrast with the findings of Signorini and Volpini (2021), where fully recycled cylindrical PET-PE fibres obtained from low-grade packaging industrial debris are investigated. In that case, a reduction of the main performance indices is reported, although the FCS is only marginally affected. This apparent contradiction may be explained, in the present case, by consideration of the peculiarities of the friction dominated failure mechanism at hand. Indeed, this failure mode heavily relies on the adhesion quality between the fibres and the matrix, which is greatly enhanced by the rough surface texture attached to recycled fibres. This surface quality is able to impart additional frictional grip with the surrounding matrix and thereby convey enhanced mechanical response to the composite (+48.6% and +42.2% for σ_{CR} and W_f, respectively).

3.3.2. Effect of ageing on bending performance

When consideration is shifted to the outcome of the ageing protocols, it appears that, under statistical significance, they all hinder mechanical performance with respect to the control group. Although this result may seem obvious, this is not always the case, see, for example, Arboleda (2014), Nobili (2016), Nobili and Signorini (2017). With respect to PC, performance of composites containing partially recycled fibres appears to decay more significantly than that of specimens containing virgin fibres, as a result of the exposure to the aggressive environments. However, it is emphasised that this applies to relative performance and does not hold for absolute performance, which remains superior in composites featuring recycled (as opposed to virgin) fibres. This aspect is particularly remarkable for HU ageing, wherein a 31.8% and 27.1% reduction in the FCS, respectively for recycled and virgin fibres, is reported. Likewise, immersion in SL leads to FCS decay for FRCC (−22.1% for virgin and −32.9% for recycled fibres), while AL and SA immersion are controversial and even brings a positive bearing on virgin fibres, although statistically weak (the opposite occurring for the dissipated energy, where recycled fibres appear to perform marginally better than control).

Similar considerations can be put forward as far as the LWC matrix is concerned. Again, SA exposure produces a limited reduction in the FCS of LWC+RPPP composites (−15.7%) and even a slight increase for LWC+PP composites. This outcome can be explained by appealing to the formation of ettringite crystals due to the presence of sulphate anions ($SO_4{}^{2-}$) in aqueous solution that can contribute, albeit marginally, in the residual hydration reactions of cement filling the porosity of the matrix and then resulting in a more compact conglomerate (Han et al., 2014). Of course, this beneficial effect is subverted in the case of exposure to sulphates for several years, which causes uncontrolled ettringite formation that can generate localised spalling. This disruptive phenomenon is regarded as *“delayed ettringite formation (DEF)”* according to the exhaustive review by Collepardi (2003). A complete overview of the results is summarised in Table 3.

3.3.3. Compression tests

Compression tests are conducted only on lightweight LWC specimens, in light of its high porosity. The mean strength curves are reported in Fig. 9.

For the sake of comparison, Figs. 10 and 11 present, respectively, peak compressive strength and dissipated energy at failure in bar-chart form, alongside ±1-standard deviation bands. Interestingly, compressive tests confirm that recycled fibres and aggregates produce superior performance compared to plain PP fibres, a result that is consistent with the outcome of bending tests. Even more striking is the fact that compressive performance of exposed specimens, especially LWC, is

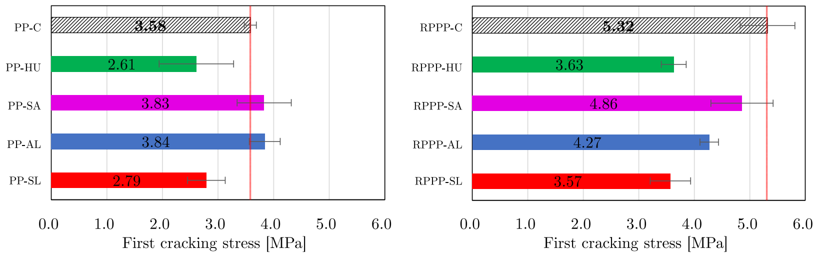

(a) PC + PP fibres (b) PC + RPPP fibres

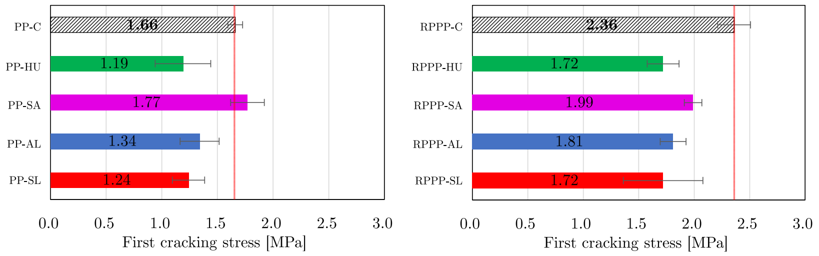

(c) LWC + PP fibres (d) LWC + RPPP fibres

Fig. 7. Mechanical performance in bending tests: first cracking stress (FCS) of plain (PC) and lightweight (LW) conglomerates exposed to the aggressive environments.

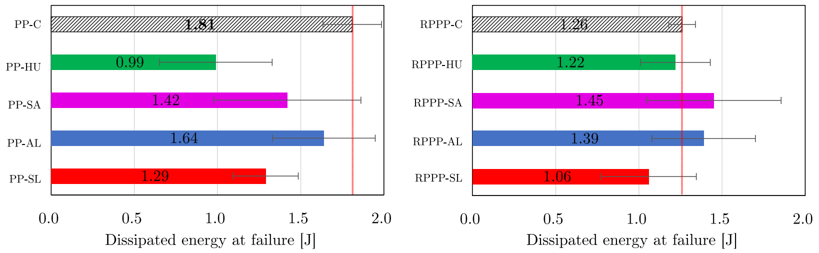

(a) PC + PP fibres (b) PC + RPPP fibres

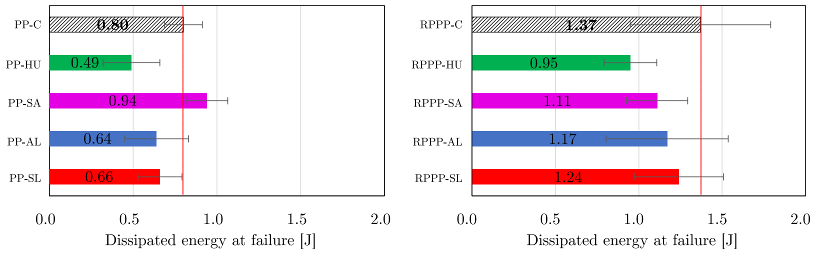

(c) LWC + PP fibres (d) LWC + RPPP fibres

Fig. 8. Mechanical performance in bending tests: energy dissipated at failure for plain (PC) and lightweight (LW) conglomerates exposed to the aggressive environments.

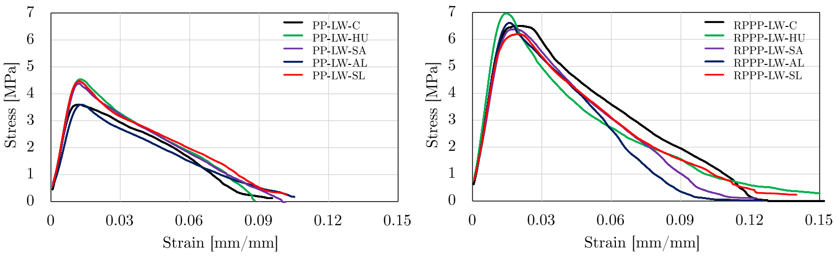

(c) LWC + PP fibres (d) LWC + RPPP fibres

Fig. 9. Strength curves in compression of lightweight concrete (LWC) exposed to aggressive environments, with respect to the control group (C).

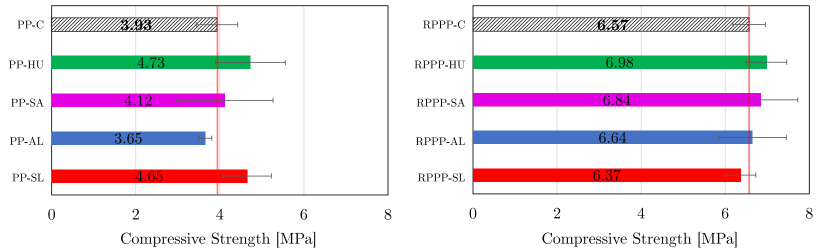

(c) LWC + PP fibres (d) LWC + RPPP fibres

Fig. 10. Compressive strength (CS) of lightweight concrete (LWC) subjected to the aggressive environments, compared to the control group (C).

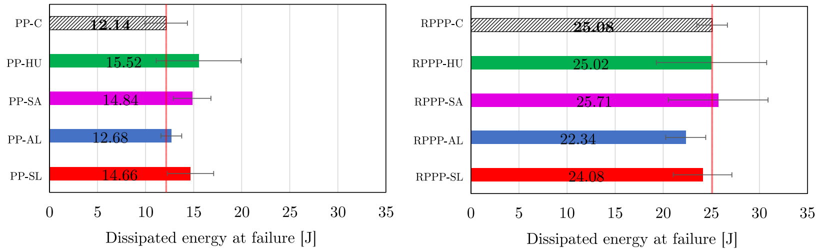

(c) LWC + PP fibres (d) LWC + RPPP fibres

Fig. 11. Dissipated mechanical energy at failure in compression (W) of lightweight concrete (LWC) exposed to the aggressive environments, compared to the control group (C).

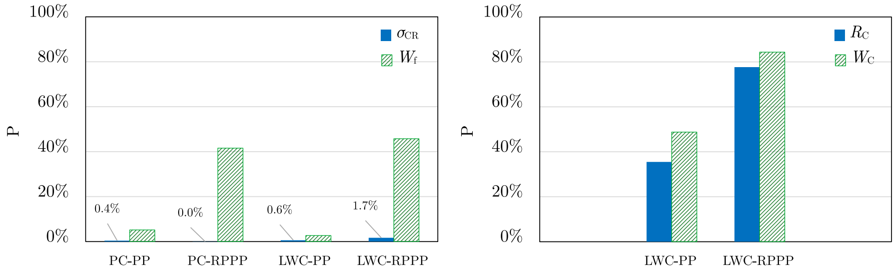

(a) P-value for bending tests (b) P-value for compression tests

Fig. 12. ANOVA test p-value for all aggressive environments vs the control group for strength and dissipated energy at failure in bending (a) and compression (b). This value expresses the probability that groups are really samplings belonging to the same population.

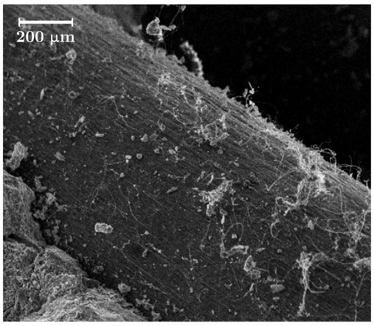

Fig. 13. Rough surface of partially recycled fibres after failure in bending. This surface finishing requires more work during the crack-opening stage, and thereby enhances toughness of FRCC.

much in line if not superior to than that of the control group, regardless of the aggressive agent.

As summarised in Table 4, only the alkaline environment (AL) induces a slight decay in the peak strength of LWC with virgin PP fibres as well as in the toughness of LWC with recycled fibres. However, such reductions are slim and comparable with data scattering width, as expressed by the standard deviation bands, and therefore may be disregarded as statistically insignificant. To better focus on this point, a statistical analysis is hereinafter presented in the form of ANOVA test.

4. Discussion and statistical analysis

To better assess the experimental data previously presented, a one-way ANalysis Of VAriance (ANOVA) test is carried out, the outcome of which is provided in Table 5. This statistical procedure is widely accepted and established and its purpose is to assess variance between σ_B and within σ_W the samplings, in order to infer the probability that groups really express an underlying phenomenon or, rather, are induced by normal fluctuations due to sampling (null hypothesis). Indeed, for the global variance σ we have

$$\sigma^2 = \sigma_W^2 + \sigma_B^2, \tag{1}$$

where

$$\sigma_B^2 = \sum_{g=1}^{G} \sigma_g^2 \frac{n_g - 1}{n - 1}, \tag{2}$$

$$\sigma_W^2 = \sum_{g=1}^{G} (\mu_g - \mu)^2 \frac{n_g}{n - 1}, \tag{3}$$

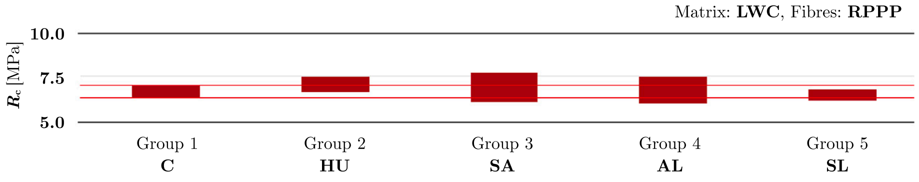

(a) Test *i* (P=77.7%)

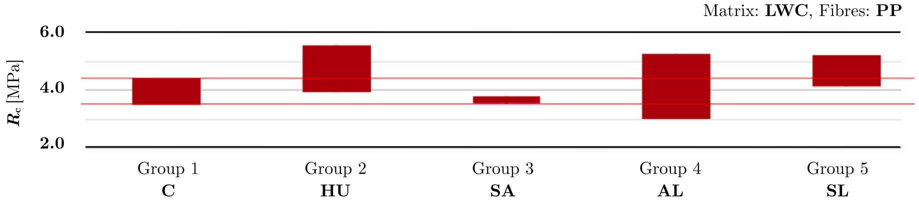

(b) Test *ii* (P=35.5%)

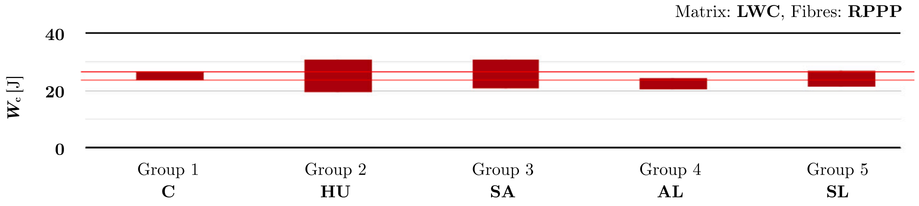

(c) Test *iii* (P=84.4%)

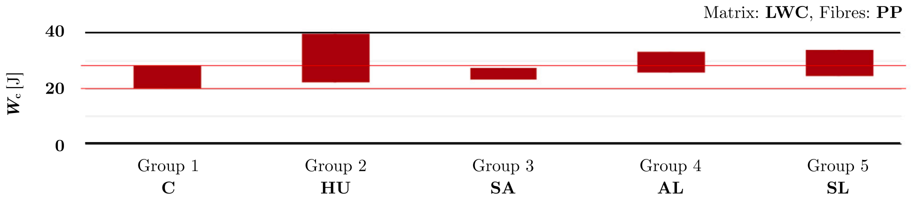

(d) Test *iv* (P=48.8%)

Fig. A.1. ANOVA test results for different group arrangements within and across in LWC matrix under compression. The single label refers to the numbering of Table 5 associated with its specific probability that the null hypothesis is verified.

Table 3
Main performance indices of FRCC retrieved from bending tests.

Matrix	Label	$\sigma_{\rm CR}$ [MPa]			$W_{\rm f}$ [J]		
		μ	ς	Δ[%]	μ	ς	Δ[%]
PC	**PP-C**	**3.58**	**0.11**	–	**1.81**	**0.18**	–
	PP-HU	2.61	0.67	−27	0.99	0.34	−45
	PP-SA	3.83	0.49	+7	1.42	0.44	−22
	PP-AL	3.84	0.28	+7	1.64	0.31	−9
	PP-SL	2.79	0.34	−22	1.29	0.20	−29
	RPPP-C	**5.32**	**0.49**	–	**1.26**	**0.08**	–
	RPPP-HU	3.63	0.22	−32	1.22	0.21	−3
	RPPP-SA	4.86	0.56	−9	1.45	0.41	+15
	RPPP-AL	4.27	0.17	−20	1.39	0.31	+10
	RPPP-SL	3.57	0.36	−32	1.06	0.29	−16
LWC	**PP-C**	**1.66**	**0.07**	–	**0.80**	**0.11**	–
	PP-HU	1.19	0.25	−28	0.49	0.17	−39
	PP-SA	1.77	0.15	+7	0.94	0.12	+18
	PP-AL	1.34	0.18	−19	0.64	0.19	−20
	PP-SL	1.24	0.14	−25	0.66	0.13	−18
	RPPP-C	**2.36**	**0.15**	–	**1.37**	**0.42**	–
	RPPP-HU	1.72	0.14	−27	0.95	0.16	−31
	RPPP-SA	1.99	0.08	−16	1.11	0.18	−19
	RPPP-AL	1.81	0.12	−23	1.17	0.37	−15
	RPPP-SL	1.72	0.36	−27	1.24	0.27	−9

Table 4
Main performance indices of LWC retrieved from compressive testing.

Matrix	Label	$R_{\rm c}$ [MPa]			$W_{\rm c}$ [J]		
		μ	ς	Δ[%]	μ	ς	Δ[%]
LWC	**PP-C**	**3.93**	**0.49**	–	**12.14**	**2.2**	–
	PP-HU	4.73	0.83	+20	15.52	4.42	+28
	PP-SA	4.12	1.14	+5	14.84	1.96	+22
	PP-AL	3.65	0.16	−7	12.68	1.08	+4
	PP-SL	4.65	0.58	+18	2.42	0.16	+20.8
	RPPP-C	**6.57**	**0.39**	–	**25.08**	**1.58**	–
	RPPP-HU	6.98	0.48	+6	25.02	5.73	–
	RPPP-SA	6.84	0.88	+4	25.71	5.18	+3
	RPPP-AL	6.64	0.81	+1	22.34	2.08	+11
	RPPP-SL	6.37	0.36	−3	24.08	3.05	−4

and $g = 1 \dots G$ ranges within the sampling groups, each encompassing n_g elements such that $n = \sum_{g=1}^{G} n_g$, μ_g is the mean of group g, while μ is the global mean. In the case of null hypothesis, variation within the sampling groups is higher than (or comparable to) that among the groups, meaning that there is no statistically significant distinction among them. This approach is also adopted and discussed in previous studies regarding the durability of composite materials, see, for example, Nobili (2016), Nobili and Signorini (2017), Tanyildizi (2021). The ANOVA test on compression data confirms that ageing effects appear marginal if recycled fibres and aggregates are considered,

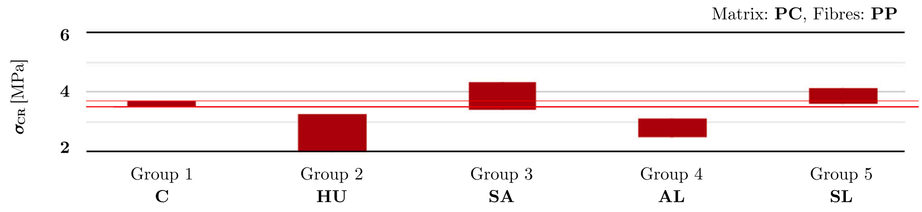

(e) Test v (P=0.4%)

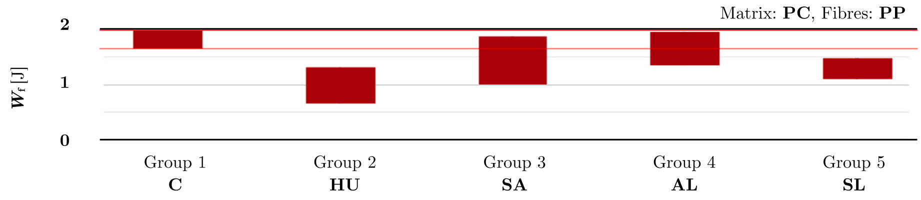

(f) Test $xiii$ (P=5.2%)

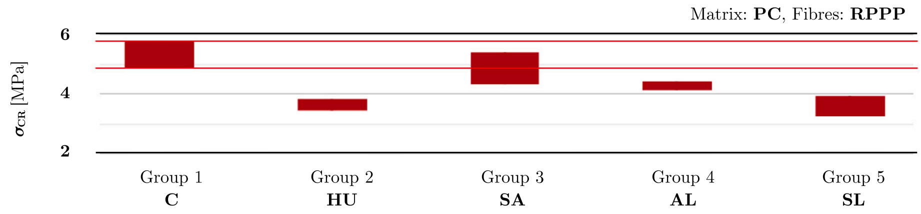

(g) Test vii (P=0.02%)

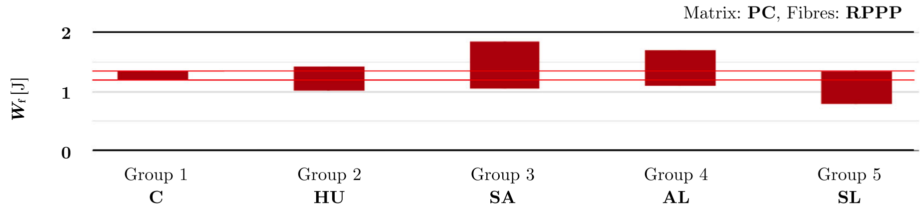

(h) Test xv (P=41.6%)

Fig. A.2. ANOVA test results for different group arrangements within and across in PC matrix under bending. The single label refers to the numbering of Table 5 associated with its specific probability that the null hypothesis is verified.

both in terms of strength and toughness. Indeed, the p-value scores 77.7% and 84.4%, respectively for strength and toughness of LWC (Fig. 12(b)). The situation is much less clear-cut for PP virgin fibres, whose p-value is 35.5% for compressive strength R_C and close to 50% for toughness W. This suggests weak statistical significance for the slight improvement in strength and energy dissipation as a result of exposure to the aggressive environments. Nonetheless, this outcome appears remarkable in consideration of the fact that all aggressive protocols (four, plus the reference) are assessed together and therefore behave in similar fashion.

This picture of (almost) uniform resistance in compression is reversed when data from bending tests are considered, as the bar-chart of Fig. 12(a) reveals. Indeed, we see that strong statistical significance is attached to the performance decay associated to the exposure to the aggressive environments, at least in terms of FCS. Table 5 gathers the results from different group combinations in the ANOVA test, for a graphical representation of which one is referred to Figs. A.1–A.3 in Appendix. With regard to the bending properties, a few interesting remarks can be put forward:

- variations of FCS among the C, SA and AL groups appear little significant in the case of PC with virgin PP fibres, which suggests these aggressive environments are not damaging the system in a significant manner. This analysis puts emphasis on the detrimental effect of HU and SL exposure.
- In contrast, statistical significance is well warranted for PC with recycled fibres, that seem consistently vulnerable.
- When recycled rubber aggregates are considered in LWC, all aggressive environments are damaging, which supports the idea that it is really the matrix, as opposed to the fibres, that determines the ageing properties (see Nobili (2016)).
- As expected, owing to larger data scattering attached to energy considerations, statistical significance is generally weaker in terms of energy dissipation;
- remarkably, the adoption of recycled fibres in LWC strongly weakens statistical significance of the detrimental effect of exposure in terms of energy dissipation.

Combining data from mechanical testing and SEM analysis of the bare fibre surface (see Fig. 13, which evidences good stability of the constituent polymer materials to the aggressive environments), it can be argued that ageing mainly affects the quality of the fibre-to-matrix interphase. This, in turn, is essentially responsible for the specimen toughness in bending, because the leading failure mechanism in the composite is friction-based, via pull-out of the fibres from the matrix (Di Maida et al., 2018; Signorini et al., 2021). In this respect, damage at the interphase becomes more detrimental when toughness of FRCC reinforced with PP fibres is considered. Indeed, this outcome can be ascribed to the constituently inherited roughness of recycled fibres,

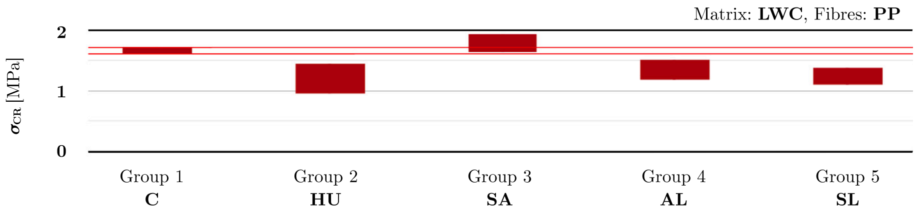

(i) Test *ix* (P=0.6%)

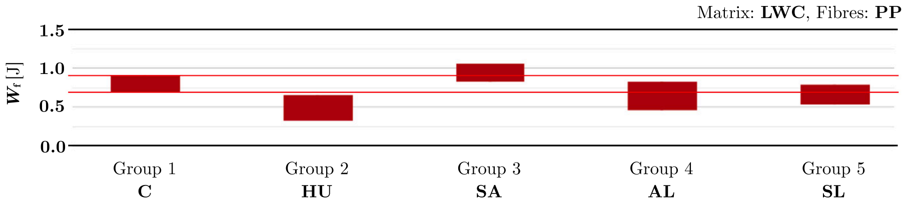

(j) Test *xvii* (P=2.7%)

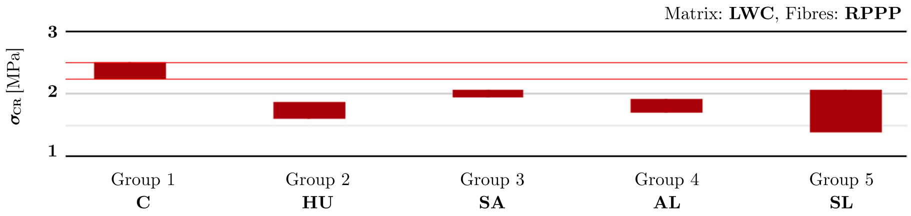

(l) Test *xi* (P=1.7%)

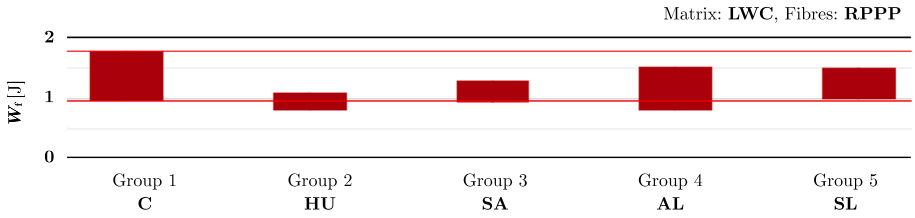

(k) Test *xix* (P=45.8%)

Fig. A.3. ANOVA test results for different group arrangements within and across in LWC matrix under bending. The single label refers to the numbering of Table 5 associated with its specific probability that the null hypothesis is verified.

which works during the crack-opening stage regardless of chemical adhesion, as shown in the magnified image of Fig. 13. The latter may be compared with the corresponding Fig. 5(a) presented by Signorini et al. (2020), that shows an extremely even and smooth surface for virgin PP fibres. In compression, this surface roughness plays a minor role in determining the mechanical response of the composite, which results in high P-values emerging from the ANOVA analysis, very close to 1, especially when recycled fibres are adopted. As already pointed out, the addition of recycled rubber-like aggregates in the mix is generally responsible for high porosity in the matrix (the particle size of the crumb rubber aggregates is coarser than that of sand) and its lightweight character. In the face of this positive outcome, the matrix becomes more susceptible to the penetration of the aggressive solution, which weakens the interphase with the fibres. However, this detrimental effect is unexpectedly mild, all the more in compression.

5. Conclusions

In this paper, we investigate long-term mechanical performance of fibre-reinforced cementitious composites (FRCC) exposed to accelerated ageing protocols simulating aggressive environmental conditions (namely distilled water, saline, acid, and alkaline solutions). Two different embedding matrices are considered: on the one hand, a standard out-of-the-shelf Portland-cement-based concrete for screeds (PC) and on the other, a cement-based lightweight concrete (LWC) where natural sand has been partly replaced with rubber recycled aggregates (RRA), as a more sustainable solution for screed manufacturing. Besides, two different synthetic macro-fibres are considered, namely virgin PP and a partially recycled blend of PP and PET retrieved from post-industrial waste treatment of the food-packaging sector. Performance is assessed in three-point bending (3PBT) and monotonic compression (MCT) tests. A one-way analysis of variance (ANOVA) is used to assess the statistical significance of the results and helps setting the spotlight on the actual damaging mechanism induced by ageing. The following conclusions can be drawn:

- Remarkably, FRCC with recycled fibres performs significantly better than that with virgin PP and this improvement is sustained with both matrices.
- A scanning electron microscopy (SEM) analysis evidences that no visible damage is evident on the fibres surface after 30 day exposure, contrarily to what generally observed by Won et al. (2010) for PET fibres. This indicates that the recycled blends considered in the present contribution exhibit significant chemical inertness and stability, which supports their application in concrete.
- As clearly highlighted by the ANOVA analysis, aggressive environment exposure mainly impacts on bending performance of

Table 5
One-way analysis of variance (F = Fisher–Snedecor ratio; P = probability that the considered specimens belong to the same population).

PI	Matrix	Fibres	Test	Groups	F	P [%]
R_c	LWC	RPPP	*i*	all	0.440	77.7
	LWC	PP	*ii*	all	1.240	35.5
W_c	LWC	RPPP	*iii*	all	0.340	84.4
	LWC	PP	*iv*	all	0.921	48.8
σ_{CR}	PC	PP	*v*	all	6.656	0.4
	PC	PP	*vi*	C, SA, AL	0.390	69.1
	PC	RPPP	*vii*	all	12.744	≤0.1
	PC	RPPP	*viii*	C, SA, AL	4.509	5.5
	LWC	PP	*ix*	all	6.441	0.6
	LWC	PP	*x*	C, SA, AL	6.812	3.7
	LWC	RPPP	*xi*	all	4.492	1.7
	LWC	RPPP	*xii*	C, SA, AL	17.29	0.2
W_f	PC	PP	*xiii*	all	3.124	5.2
	PC	PP	*xiv*	C, SA, AL	0.828	47.5
	PC	RPPP	*xv*	all	1.057	41.6
	PC	RPPP	*xvi*	C, SA, AL	0.210	81.6
	LWC	PP	*xvii*	all	4.162	2.71
	LWC	PP	*xviii*	C, SA, AL	2.954	14.2
	LWC	RPPP	*xix*	all	0.967	45.8
	LWC	RPPP	*xx*	C, SA, AL	0.466	64.5

FRCC, as opposed to compression, suggesting that the detrimental effect is mainly restricted to the interphase between the fibres and the matrix. Indeed, during the crack-opening stage in bending, the driving resisting mechanism is provided by friction at the interphase.

- In this regard, partially recycled fibres offer better mechanical performance, as a consequence of the rough surface induced by the intrinsic immiscibility of the blend constituents.
- As expected, FRCC with recycled aggregates is generally more prone to suffer from ageing, owing to the coarser particle size distribution of the RRA with respect to sand, which produces a higher porosity in the final material and lightweight. However, this performance loss is surprisingly mild.

In conclusion, this study supports the feasibility of adopting sustainable solutions in the construction industry through a wide-scope durability analysis. It endorses the use of recycled fibres and aggregates in the manufacturing of resilient construction materials for structural and non-structural screeds, which warrants solid performance over the time.

Declaration of competing interest

The authors declare that they have no known competing financial interests or personal relationships that could have appeared to influence the work reported in this paper.

Acknowledgements

This research was funded by Regione Emilia-Romagna through the POR-FESR grant titled: “Progetto IMPReSA, Impiego di Materiali Plastici da Riciclo per malte e calcestruzzi Strutturali Alleggeriti” in the framework of strategic industrial research projects (POR-FESR 2014/2020-asse 1.2.2) [CUP E81F18000310009]. Authors gratefully acknowledge PlasticFibre Srl and Dr. Igor Degli Angeli for supplying virgin as well as recycled fibres. The valuable contribution by Dr. Miriam Hanuskova and Dr. Mauro Zapparoli for particle size analysis and SEM imaging, respectively, and by Dr. Valentina Volpini and Ing. Gian Marco Macchioni for specimen manufacturing and data elaboration is gratefully recognised.

Appendix. ANOVA tests graphic visualisation

To provide a clear picture of data scattering within and among the different groups, this appendix gathers in Figs. A.1–A.3 results from various ANOVA combinations for aged and control specimens, for each matrix–fibre pairing under several performance indices, collecting data from both 3PB and compressive tests.

References

Almansa, E., Canovas, M., 1970. Design of SFRC barriers against impact of small arms projectiles. WIT Trans. Built Environ. 25.

Arboleda, D., 2014. Fabric reinforced cementitious matrix (FRCM) composites for infrastructure strengthening and rehabilitation: Characterization methods. (Ph.D. thesis). University of Miami, Open Access Dissertation. Paper 1282.

ASTM D 1141, 2013. Standard practice for the preparation of substitute ocean water. American Society for Testing and Materials International.

Benosman, A., Mouli, M., Taibi, H., Belbachir, M., Senhadji, Y., 2011. Resistance of polymer (PET)-mortar composites to aggressive solutions. In: International Journal of Engineering Research in Africa. 5, Trans Tech Publ, pp. 1–15.

Benosman, A.S., Mouli, M., Taibi, H., Belbachir, M., Senhadji, Y., Bahlouli, I., Houivet, D., 2013. Studies on chemical resistance of PET-mortar composites: microstructure and phase composition changes.

Bentur, A., Mindess, S., 2006. Fibre Reinforced Cementitious Composites. CRC Press.

Collepardi, M., 2003. A state-of-the-art review on delayed ettringite attack on concrete. Cem. Concr. Compos. 25 (4–5), 401–407.

Di Maida, P., Sciancalepore, C., Radi, E., Bondioli, F., 2018. Effects of nano-silica treatment on the flexural post cracking behaviour of polypropylene macro-synthetic fibre reinforced concrete. Mech. Res. Commun. 88, 12–18.

Dong, X., Ding, Y., Wang, T., 2008. Spalling and mechanical properties of fiber reinforced high-performance concrete subjected to fire. J. Wuhan University of Technology-Mater. Sci. Ed. 23 (5), 743–749.

Foti, D., 2013. Use of recycled waste PET bottles fibers for the reinforcement of concrete. Compos. Struct. 96, 396–404.

Fraternali, F., Ciancia, V., Chechile, R., Rizzano, G., Feo, L., Incarnato, L., 2011. Experimental study of the thermo-mechanical properties of recycled PET fiber-reinforced concrete. Compos. Struct. 93 (9), 2368–2374.

Gu, L., Ozbakkaloglu, T., 2016. Use of recycled plastics in concrete: A critical review. Waste Manage. 51, 19–42.

Han, P., Liu, X., Bai, X.-h., 2014. Effect of sodium sulfate on strength and micropores of cemented soil. Rock Soil Mech. 35 (9), 2555–2561.

Holmes, N., Browne, A., Montague, C., 2014. Acoustic properties of concrete panels with crumb rubber as a fine aggregate replacement. Constr. Build. Mater. 73, 195–204.

Larsen, E.S., Krenchel, H., 1990. Durability of FRC-materials. MRS Online Proc. Libr. Arch. 211.

Li, X., Ling, T.-C., Mo, K.H., 2020. Functions and impacts of plastic/rubber wastes as eco-friendly aggregate in concrete–a review. Constr. Build. Mater. 240, 117869.

Luna, C.B.B., Araújo, E.M., Siqueira, D.D., Morais, D.D.d.S., Filho, E.A.d.S., Fook, M.V.L., 2020. Incorporation of a recycled rubber compound from the shoe industry in polystyrene: effect of SBS compatibilizer content. J. Elastomers Plast. 52 (1), 3–28.

Marcos-Meson, V., Michel, A., Solgaard, A., Fischer, G., Edvardsen, C., Skovhus, T.L., 2018. Corrosion resistance of steel fibre reinforced concrete-a literature review. Cem. Concr. Res. 103, 1–20.

Marinelli, S., Butturi, M.A., Rimini, B., Gamberini, R., Sellitto, M.A., 2021. Estimating the circularity performance of an emerging industrial symbiosis network: The case of recycled plastic fibers in reinforced concrete. Sustainability 13 (18), 10257.

Marthong, C., Sarma, D.K., 2016. Influence of PET fiber geometry on the mechanical properties of concrete: an experimental investigation. Eur. J. Environ. Civil Eng. 20 (7), 771–784.

Meddah, M., Bencheikh, M., 2009. Properties of concrete reinforced with different kinds of industrial waste fibre materials. Constr. Build. Mater. 23 (10), 3196–3205.

Medina, N.F., Flores-Medina, D., Hernández-Olivares, F., 2016. Influence of fibers partially coated with rubber from tire recycling as aggregate on the acoustical properties of rubberized concrete. Constr. Build. Mater. 129, 25–36.

Medina, N.F., Medina, D.F., Hernández-Olivares, F., Navacerrada, M., 2017. Mechanical and thermal properties of concrete incorporating rubber and fibres from tyre recycling. Constr. Build. Mater. 144, 563–573.

Naaman, A.E., Shah, S.P., 1976. Pull-out mechanism in steel fiber-reinforced concrete. J. Struct. Div. 102 (8), 1537–1548.

Nobili, A., 2016. Durability assessment of impregnated glass fabric reinforced cementitious matrix (GFRCM) composites in the alkaline and saline environments. Constr. Build. Mater. 105, 465–471.

Nobili, A., Signorini, C., 2017. On the effect of curing time and environmental exposure on impregnated carbon fabric reinforced cementitious matrix (CFRCM) composite with design considerations. Composites B 112, 300–313.

Ochi, T., Okubo, S., Fukui, K., 2007. Development of recycled PET fiber and its application as concrete-reinforcing fiber. Cem. Concr. Compos. 29 (6), 448–455.

Peng, G.-F., Yang, W.-W., Zhao, J., Liu, Y.-F., Bian, S.-H., Zhao, L.-H., 2006. Explosive spalling and residual mechanical properties of fiber-toughened high-performance concrete subjected to high temperatures. Cem. Concr. Res. 36 (4), 723–727.

Rider, R., Heidersbach, R., 1980. Degradation of metal-fiber-reinforced concrete exposed to a marine environment. In: Corrosion of Reinforcing Steel in Concrete. ASTM International.

Signorini, C., Nobili, A., 2021. Comparing durability of steel reinforced grout (SRG) and textile reinforced mortar (TRM) for structural retrofitting. Mater. Struct. 54 (3), 1–15.

Signorini, C., Sola, A., Malchiodi, B., Nobili, A., 2021. Highly dissipative fiber-reinforced concrete for structural screeds. J. Mater. Civ. Eng. http://dx.doi.org/10.1061/(ASCE)MT.1943-5533.0004160.

Signorini, C., Sola, A., Malchiodi, B., Nobili, A., Gatto, A., 2020. Failure mechanism of silica coated polypropylene fibres for fibre reinforced concrete (FRC). Constr. Build. Mater. 236, 117549.

Signorini, C., Volpini, V., 2021. Mechanical performance of fiber reinforced cement composites including fully-recycled plastic fibers. Fibers 9 (3), 16.

Silva, D., Betioli, A., Gleize, P., Roman, H., Gomez, L., Ribeiro, J., 2005. Degradation of recycled PET fibers in portland cement-based materials. Cem. Concr. Res. 35 (9), 1741–1746.

Sorzia, A., Lanzoni, L., Radi, E., 2019. Pullout modelling of viscoelastic synthetic fibres for cementitious composites. Compos. Struct. 223, 110898.

Tanyildizi, H., 2021. Investigation of mechanical properties of polymer impregnated concrete containing polypropylene fiber by taguchi and ANOVA methods. Revis. de la Constr. 20 (1), 52–61.

Tardiff Jr., G., 1973. Fracture mechanics of brittle matrix ductile fiber composites. Eng. Fract. Mech. 5 (1), 1–10.

UNI EN 1015-11, 2007. Methods of test for mortar for masonry – Part 11: Determination of flexural and compressive strength of hardened mortar. In: Tech. Rep.. British Standards Institution-BSI and CEN European Committee for Standardization.

Wang, Y., 1995. Reuse of carpet industrial waste for concrete reinforcement. In: Disposal and Recycling of Organic and Polymeric Construction Materials. CRC Press, pp. 230–237.

Wang, J., Du, B., 2020. Experimental studies of thermal and acoustic properties of recycled aggregate crumb rubber concrete. J. Build. Eng. 32, 101836.

Whitney, J.M., Daniel, I.M., Pipes, R.B., 1982. Experimental Mechanics of Fiber Reinforced Composite Materials. Prentice Hall, p. 4.

Won, J.-P., Jang, C.-I., Lee, S.-W., Lee, S.-J., Kim, H.-Y., 2010. Long-term performance of recycled PET fibre-reinforced cement composites. Constr. Build. Mater. 24 (5), 660–665.

Yang, E.-H., Li, V.C., 2010. Strain-hardening fiber cement optimization and component tailoring by means of a micromechanical model. Constr. Build. Mater. 24 (2), 130–139.

Yin, S., Tuladhar, R., Shi, F., Combe, M., Collister, T., Sivakugan, N., 2015. Use of macro plastic fibres in concrete: A review. Constr. Build. Mater. 93, 180–188.

Zhang, P., Kang, L., Wang, J., Guo, J., Hu, S., Ling, Y., 2020. Mechanical properties and explosive spalling behavior of steel-fiber-reinforced concrete exposed to high temperature—a review. Appl. Sci. 10 (7), 2324.

Zhang, B., Poon, C.S., 2018. Sound insulation properties of rubberized lightweight aggregate concrete. J. Cleaner Prod. 172, 3176–3185.